Contribution from the Dipartimento di Chimica Inorganica e Metallorganica, Università di Milano, Centro CNR, 20133 Milano, Italy, Dipartimento di Chimica, Università di Firenze, 50121 Firenze, Italy, and Central Research Institute for Chemistry, Hungarian Academy of Sciences, H-1525 Budapest, Hungary

Iron(III) Tyrosinate Models. Synthesis and Spectroscopic and Stereochemical Studies of Iron(III) Complexes of *N*-Salicylidene-L-amino Acids[1]

L. Casella,*† M. Gullotti,† A. Pintar,† L. Messori,‡ A. Rockenbauer,§ and M. Györ§

Received August 7, 1986

A series of iron(III) complexes of the imines of L-amino acids derived from salicylaldehyde, Fe(sal-L-aa)Cl (aa = ala, val, phe, his), and the corresponding complex obtained from histamine, Fe(sal-him)Cl_2, have been prepared and characterized by various spectroscopic techniques. The complexes are high spin and have five- or six-coordinate structures. They generally exist in solution as equilibrium mixtures of monomeric and dimeric forms, the ratio of which depends upon the solvent and the presence of externally added ligands. Information on the two species has been obtained by combined ESR and NMR measurements. The NMR spectra, in particular, show two sets of paramagnetically shifted proton resonances that can be attributed to the salicylaldimine protons of the two species, the dimeric species exhibiting smaller NMR shifts than the monomeric species. The optical spectra of the complexes are largely determined by transitions originating in the iron salicylaldiminate chromophore. An assignment of the low-energy phenolate to iron(III) LMCT bands has been made possible by the analysis of the electronic and CD spectra of the complexes and their adducts with donor bases and by MO calculations performed on the ligand analogues *N*-methylsalicylaldiminate and *p*-methylphenolate anions. The spectral features of the iron complexes and their adducts have been discussed in relation to those of the iron tyrosinate proteins. Of particular relevance are the adducts of the complexes with catecholate anions since their spectral properties often mimic those of the enzyme–substrate complexes of the catechol dioxygenases.

Introduction

The iron tyrosinate proteins[2] are a heterogeneous group of non-heme iron proteins including the transferrins,[3] the catechol dioxygenases,[4] and the purple acid phosphatases.[5] In spite of their diverse functions these proteins display, as a common spectral feature, a moderately intense absorption band in the range 400–600 nm that dominates the visible spectrum and originates from a tyrosinate to iron(III) charge-transfer transition. The position and intensity of this band are sensitive to the ligand environment of iron(III) and, in particular, undergo significant changes on adding a variety of external ligands or potential substrates to the proteins.[2] Only limited information is available on the nature of the protein ligands other than tyrosine involved in binding to iron(III), except for the frequent involvement of histidine imidazole groups.[2] Hence the importance of model studies[6-13] that can provide useful data to improve our understanding of spectra–structure correlations for the protein metal sites.

In this paper we wish to report a series of chiral iron(III) complexes with ligands derived from the condensation of salicylaldehyde and L-amino acids, **1** and **2**, or histamine, **3**, that extends

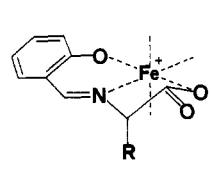

1

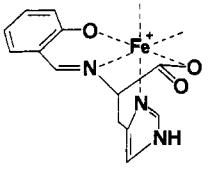

2

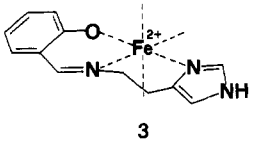

3

the range of available model studies on iron(III) salicylaldimine complexes to include ligand residues that are potential donor groups of iron(III) in the proteins, e.g. the imidazole and carboxylate groups of the amino acid residues. Systems of types **1–3** are particularly convenient for the investigation of the effect on the spectra of adduct formation with additional ligand molecules, since both equatorial and axial coordination positions are in principle available for the added ligands. Preliminary spectral results on some of these systems have been reported recently.[14]

Experimental Section

Physical Measurements. Elemental analyses were from the microanalytical laboratory of the University of Milano. Infrared spectra were recorded on a Nicolet MX-1E FT-IR instrument using a 2-cm^{-1} standard resolution. Electronic spectra were recorded on a Perkin-Elmer Lambda-5 spectrophotometer and circular dichroism spectra on a Jasco-500 C dichrograph; optical cells fitted with Schlenk connections were employed for recording electronic and CD spectra of solutions under a nitrogen atmosphere. Paramagnetic ^1H NMR spectra were obtained on a Bruker WP-80 (80 MHz) or a Bruker CXP spectrometer operating at 90 MHz, both using the pulsed Fourier transform technique; all chemical

† Università di Milano.
‡ Università di Firenze.
§ Hungarian Academy of Sciences.

(1) Coordination Modes of Histidine. 10. For part 9 see ref 18.
(2) Que, L., Jr. *Coord. Chem. Rev.* **1983**, *50*, 73–108.
(3) (a) Aisen, P.; Listowsky, I. *Annu. Rev. Biochem.* **1980**, *49*, 357–393. (b) Chasteen, N. D. *Adv. Inorg. Biochem.* **1983**, *5*, 201–233.
(4) (a) Nozaki, M. In *Molecular Mechanisms of Oxygen Activation*; Hayashi, O., Ed.; Academic: New York, 1974; pp 135–165. (b) Nozaki, M. *Top. Curr. Chem.* **1979**, *78*, 145–186. (c) Que, L., Jr. *Adv. Inorg. Biochem.* **1983**, *5*, 167–199. (d) Que, L., Jr. *J. Chem. Educ.* **1985**, *62*, 938–943.
(5) (a) Antanaitis, B. C.; Aisen, P. *Adv. Inorg. Biochem.* **1983**, *5*, 111–136. (b) Antanaitis, B. C.; Aisen, P.; Lilienthal, H. R. *J. Biol. Chem.* **1983**, *258*, 3166–3172. (c) Lauffer, R. B.; Antanaitis, B. C.; Aisen, P.; Que, L., Jr. *Ibid.* **1983**, *258*, 14212–14218.
(6) Gaber, B. P.; Miskowski, V.; Spiro, T. G. *J. Am. Chem. Soc.* **1974**, *96*, 6868–6873.
(7) Ainscough, E. W.; Brodie, A. M.; Plowman, J. E.; Brown, K. L.; Addison, A. W.; Gainsford, A. R. *Inorg. Chem.* **1980**, *19*, 3655–3663.
(8) (a) Lauffer, R. B.; Heistand, R. H. II; Que, L., Jr. *J. Am. Chem. Soc.* **1981**, *103*, 3947–3949. (b) Heistand, R. H. II; Lauffer, R. B.; Fikrig, E.; Que, L., Jr. *Ibid.* **1982**, *104*, 2789–2796. (c) White, L. S.; Nilsson, P. V.; Pignolet, L. H.; Que, L., Jr. *Ibid.* **1984**, *106*, 8312–8313. (d) Roe, A. L.; Schneider, D. J.; Mayer, R. J.; Pyrz, J. W.; Widom, I. W.; Que, L., Jr. *Ibid.* **1984**, *106*, 1676–1681. (e) Pyrz, I. W.; Roe, A. L.; Stern, L. J.; Que, L., Jr. *Ibid.* **1985**, *107*, 614–620.
(9) (a) Heistand, R. H. II; Roe, A. L.; Que, L., Jr. *Inorg. Chem.* **1982**, *21*, 676–681. (b) Lauffer, R. B.; Heistand, R. H. II; Que, L., Jr. *Ibid.* **1983**, *22*, 50–55. (c) Davis, J. C.; Kung, W.-J.; Averill, B. A. *Ibid.* **1986**, *25*, 394–396.
(10) Koch, S. A.; Millar, M. *J. Am. Chem. Soc.* **1982**, *104*, 5255–5257.
(11) Nishida, Y.; Shimo, H.; Kida, S. *J. Chem. Soc., Chem. Commun.* **1984**, 1611–1612.
(12) (a) Weller, M. G.; Weser, U. *J. Am. Chem. Soc.* **1982**, *104*, 3752–3754. (b) Weller, M. G. In *The Coordination Chemistry of Metalloenzymes*; Bertini, I., Drago, R. S., Luchinat, C., Eds.; D. Reidel: Dordrecht, The Netherlands, 1983; pp 273–278. (c) Weller, M. G.; Weser, U. *Inorg. Chim. Acta* **1985**, *107*, 243–245.
(13) (a) Pecoraro, V. L.; Harris, W. R.; Carrano, C. J.; Raymond, K. *Biochemistry* **1981**, *20*, 7033–7039. (b) Patch, M. G.; Simolo, K. P.; Carrano, C. J. *Inorg. Chem.* **1983**, *22*, 2630–2634. (c) Carrano, C. J.; Spartalian, K.; Rao, G. V. N. A.; Pecoraro, V. L.; Sundaralingam, M. *J. Am. Chem. Soc.* **1985**, *107*, 1651–1658.
(14) Casella, L.; Gullotti, M.; Pintar, A. *Rev. Port. Quim.* **1985**, *27*, 285–286.

0020-1669/87/1326-1031$01.50/0

Table I. Elemental Analyses of the Iron(III) Complexes

compound	formula	anal., % calcd C	calcd H	calcd N	found C	found H	found N
Fe(sal-L-ala)Cl·H_2O	$FeC_{10}H_9NO_3Cl·H_2O$	39.95	3.69	4.66	39.32	4.09	4.46
Fe(sal-L-val)Cl·H_2O	$FeC_{12}H_{13}NO_3Cl·H_2O$	43.84	4.60	4.26	43.45	4.85	4.06
Fe(sal-L-phe)Cl·H_2O	$FeC_{16}H_{15}NO_3Cl·H_2O$	50.75	4.53	3.70	50.70	4.42	3.50
Fe(sal-L-his)Cl·H_2O	$FeC_{13}H_{11}N_3O_3Cl·H_2O$	42.59	3.57	11.46	42.31	4.08	11.39
Fe(sal-him)Cl_2·0.5C_2H_5OH	$FeC_{12}N_3OCl_2·0.5C_2H_5OH$	42.90	4.15	11.55	43.22	3.69	11.31
Fe(sal-L-val)(bpy)Cl	$FeC_{22}H_{21}N_3O_3Cl$	56.58	4.54	9.01	56.34	4.72	9.05
Fe(sal-L-his)(bpy)Cl	$FeC_{23}H_{19}N_5O_3Cl$	54.71	3.80	13.88	53.30	4.00	13.26

shift data were referenced to Me_4Si with downfield shifts taken as positive. Electron spin resonance spectra were obtained at X-band frequencies on Varian E-109 and JEOL JES-FE/3X spectrometers. Magnetic susceptibility measurements were measured at room temperature with a Cahn 1000 electrobalance. Tetrakis(thiocyanato)mercury cobaltate was used as a susceptibility standard and the diamagnetic corrections were estimated with use of the appropriate Pascal constants.

Preparations.[15] The complexes Fe(sal-L-ala)Cl, Fe(sal-L-val)Cl, and Fe(sal-L-phe)Cl were prepared according to the following procedure. Salicylaldehyde (5 mmol) and the amino acid (5 mmol) were refluxed in ethanol–water (50 mL, 9/1 v/v) for 30 min. To the cooled yellow solution was added solid $FeCl_3·6H_2O$ (5mmol) with stirring, followed by methanolic ~1 N sodium hydroxide (10 mmol). The dark, brownish violet solution was stirred for several hours at room temperature and then evaporated to dryness under vacuum. The solid residue was treated several times with small volumes of 1:1 ethanol–toluene and rotary evaporated to dryness in order to eliminate water as much as possible. The solid residue was finally treated with toluene–ethanol (100 mL, 4/1 v/v) and filtered to eliminate sodium chloride. The filtrate was concentrated under vacuum, and the product was precipitated by dropwise addition of hexane as a violet powder. This was collected by filtration and dried under vacuum. The complexes Fe(sal-L-his)Cl and Fe(sal-him)Cl_2 were obtained similarly except that the ligand solutions were prepared only by warming, and not by refluxing, salicylaldehyde and the histidine derivative in aqueous ethanol to prevent cyclization of the Schiff base.[16] Also, for Fe(sal-L-his)Cl the final addition of hexane was not necessary because the product precipitated from the concentrate toluene–ethanol solution.

The adducts Fe(sal-L-val)(bpy)Cl and Fe(sal-L-his)(bpy)Cl were obtained by stirring the iron(III) complex (~100mg) and α,α'-bipyridyl (1:2 molar ratio) in methanol (~20 mL) for 2 h. After evaporation to dryness of the solution, toluene was added to the residue and the product was collected by filtration. The adduct was stirred again in toluene to remove traces of free α,α'-bipyridyl and then filtered and dried under vacuum. The elemental analyses are collected in Table I.

Results

Synthesis and Characterization.[15] The iron complexes **1–3** were prepared, as for related systems,[16–18] by metal ion template condensation of salicylaldehyde and the amino acid derivative. Compared with that for the corresponding zinc(II),[16] copper(II),[17] and cobalt(II)[18] complexes, a somewhat more sluggish isolation procedure was required, due to the inherent difficulty in crystallizing the iron complexes, particularly when trace amounts of water are present in the reaction medium. Some water is retained by the complexes in the solid state, as indicated by ν(OH) bands at 3300–3400 cm^{-1} in the IR spectra and elemental analyses. The imine structure of the ligands is also clearly indicated by intense and well-resolved ν(C=N) bands near 1620 cm^{-1} in the IR spectra. The other main IR bands occur at positions similar to those of related systems[16–18] and will not be discussed further here. Complete IR data have been made available as supplementary material.

In order to establish the availability of iron coordination sites to additional ligand molecules, we prepared a few adducts of representative complexes with donor bases. Adducts with α,α'-bipyridyl could be isolated easily, whereas attempted preparations of adducts with monodentate bases like pyridine or *p*-toluidine led to the isolation of the starting complexes or mixtures containing only a small fraction of the added ligands. We also tried to isolate adducts with phenolate and catecholate anions, but the analytical data of the resulting materials were not fully satisfactory.

The ferric centers of the Fe(sal-L-aa)Cl complexes are high spin, as shown by magnetic susceptibility measurements at room temperature. These correspond to μ_{eff} values in the range 5.0–5.3 μ_B for the complexes containing nonpolar amino acid side chains and 5.56 μ_B for Fe(sal-him)Cl_2, while for Fe(sal-L-his)Cl μ_{eff} = 4.44 μ_B. Some of these μ_{eff} values increase in methanol solution; for instance, we obtained 5.1 μ_B for Fe(sal-L-ala)Cl, 5.4 μ_B for Fe(sal-L-his)Cl, and 6.0 μ_B for Fe(sal-him)Cl_2 with the Evans method.[19] However, in general, it seems likely that also in solution the somewhat low values of μ_{eff} originate from molecular association. This is confirmed by the spectral behavior of the complexes to be discussed below and by conductivity measurements in various solvents, which gave unreliable Onsager plots over a concentration range. Such behavior cannot be accounted for by the establishment of simple dissociation equilibria of the type Fe(sal-L-aa)Cl $\rightleftharpoons$ Fe(sal-L-aa)$^+$ + Cl^- in solution, since the addition of an excess of chloride ions does not affect appreciably the absorption, CD, and NMR spectra of the complexes. By contrast, significant spectral changes were observed on diluting (or even on aging) solutions of the complexes in a protic solvent like methanol. The absorption spectra of the α,α'-bipyridyl adducts in dilute solution show base dissociation; to obtain stable spectra, an excess of base had therefore to be added.

Electronic and CD Spectra. The electronic spectra of the Fe(sal-L-aa)Cl complexes display several bands in the near-UV and visible regions; the absorption maxima in methanol or aqueous methanol solutions occur near 230 (ϵ = 15000–20000 M^{-1} cm^{-1}), 260 (12000–17000), 295 (~5500), and 320 nm (~5500) and in the range 490–540 nm (1100–1600). The visible band is responsible for the purple color of these complexes. Weak shoulders near 420 nm are always clearly detectable on the low-energy tail of the 320-nm band. The spectra show solvent dependence. This is partly due to solvent coordination to iron(III) but is also due to a different degree of association of the complexes in the various solvents. The spectra of complexes of type **1** in protic solvents often show significant concentration dependence, the visible band being mostly affected in these conditions. For instance, λ_{max} for Fe(sal-L-val)Cl in methanol solution shifts from 518 to 534 nm on dilution from 3×10^{-2} M to 4×10^{-4} M, with almost negligible intensity change. The absorption spectrum of the complex derived from histamine, Fe(sal-him)Cl_2, is similar to those of the derivatives of amino acids, but the visible band occurs at 582 nm and the lower energy near-UV band at 328 nm.

In order to make reliable assignments of the electronic bands, it is useful to examine the CD spectra of the complexes. In general, these spectra exhibit CD extrema or detectable shoulders in

(15) Abbreviations: *N*-salicylideneamino acidato dianion = sal-aa; condensed alaninate anion = ala; condensed valinate anion = val; condensed phenylalaninate anion = phe; condensed histidinate anion = his; condensed histamine = him; pyridine = py; α,α'-bipyridyl = bpy; imidazole = im; *p*-toluidine = tol; *o*-phenylenediamine = dab; catechol = $catH_2$; 3,5-di-*tert*-butylcatechol = $dbcatH_2$; *p*-cresol = cresH; benzoic acid = benzH, salicylic acid = salH; *N,N'*-ethylenebis(salicylideneaminato) dianion = salen.

(16) Casella, L.; Gullotti, M. *J. Am. Chem. Soc.* **1981**, *103*, 6338–6347.

(17) (a) Casella, L.; Gullotti, M.; Pasini, A.; Rockenbauer, A. *Inorg. Chem.* **1979**, *18*, 2825–2835. (b) Casella, L.; Gullotti, M.; Pacchioni, G. *J. Am. Chem. Soc.* **1982**, *104*, 2386–2396.

(18) Casella, L.; Gullotti, M. *Inorg. Chem.* **1986**, *25*, 1293–1303.

(19) Evans, D. F. *J. Chem. Soc.* 1959, 2003–2005.

Table II. Electronic Spectral Data for the Adducts of Iron(III) Complexes in Methanol Solution[a]

added ligand[b]	λ_{max}, nm (ϵ, M^{-1} cm^{-1})		
	Fe(sal-L-val)Cl	Fe(sal-L-his)Cl	Fe(sal-him)Cl_2
none	530 (1300),[c] 430 sh (970)	495 (1600), 418 (1620)	582 (1730), 430 sh (1030)
im (1:1)	500 (1200), 425 sh (1200)	480 (1650), 417 (1750)	533 (1540), 430 sh (1100)
im	480 (1200), 420 sh (1370)	478 (1650), 416 (1750)	520 (1570), 425 sh (1120)
py	496 (1350), 428 sh (1350)	486 (1680), 418 (1750)	540 (1540), 430 sh (1100)
bpy	490 (1350), 425 sh (1800)	486 (1670), 418 (1800)	543 (1480), 430 sh (1730)
tol	484 (1370), 425 sh (1400)	480 (1675), 418 (1800)	527 (1590), 425 sh (1150)
dab	480 (1430), 425 sh (1560)	478 (1680), 418 (1820)	530 (1810), 430 sh (1680)
$cres^-$	465 sh (1750), 414 (2130)[f]	477 (1970), 418 (2050)	525 (2050), 430 sh (1150)[f]
$benz^-$	470 (1960), 415 sh (2240)	484 (1700), 418 (1730)	520 (2040), 425 sh (1700)
sal^-	488 (2770), 420 sh (2140)	482 (2200), 418 (2050)	513 (2840), 425 sh (1600)
$catH^-$ (1:1)[d]	700 sh (1150), 478 (2750), 419 (2700)	700 sh (300), 476 (1700), 418 (1750)	750 sh (800), 540 (2350), 430 sh (1830)
cat^{2-} (1:1)[d]	600 sh (2380), 490 (3650), 418 (3200)	478 (1900), 417 (1920)	615 (2780), 465 sh (2830), 416 (3080)
$dbcatH^-$ (1:1)[d]	680 sh (1180), 475 (1850), 420 (1850)[e]	700 sh (570), 473 (1780), 416 (1880)	770 sh (1000), 534 (1980), 430 sh (1370)
$dbcat^{2-}$ (1:1)[d]	670 sh (1200), 470 (2030), 418 (2130)[e]	700 sh (670), 470 (1920), 414 (2170)	705 (2300), 465 (2380), 412 (2460)

[a] Concentration of iron complex $\sim 2 \times 10^{-3}$ M. [b] Unless otherwise stated the ratio of added ligand vs. iron complex was 10:1 for monodentate base and 5:1 for chelating base; the anions $cres^-$, $benz^-$ and sal^- were generated by adding 1 equiv of *t*-BuOK or methanolic NaOH to solutions containing the ligand and iron complex in a ratio of 5:1. [c] This λ_{max} varies with concentration; see text. [d] Recorded under nitrogen; the monoanions and dianions were generated by adding the corresponding amounts of *t*-BuOK to dry methanol solutions. [e] [Fe] = 7×10^{-4} M. [f] Recorded in acetonitrile.

correspondence with the absorption bands near 230, 260, 295, and 420 nm. The near-UV range of the CD spectra is dominated by an intense, negative band near 350 nm whose counterpart in the absorption spectra is only partially resolved under the broad envelope of the 320-nm band. The visible CD activity is significant only for Fe(sal-L-his)Cl, but both of the observed positive CD bands (450 and 543 nm) are appreciably displaced from the position of the absorption maximum. For the complexes derived from amino acids with nonpolar side chains, most of the residual, weak CD activity in the visible region (a band or shoulder near 450 nm and a broad band in the range 500–550 nm, both of positive sign) is due to their association forms; in fact, this CD activity progressively decreases in intensity on diluting their methanolic solutions (the CD range below 450 nm is practically unaffected by this treatment).

The electronic bands near 230 and 260 nm are due to the benzenoid $\pi \rightarrow \pi^*$ transitions, and that near 350 nm is due to the conjugated imine $\pi \rightarrow \pi^*$ transition of the salicylaldimine residue. Similar bands are observed in the spectra of *N*-salicylidene-L-amino acid complexes with divalent metal ions,[16-18] but all of them appear slightly blue shifted in the iron(III) systems for the increase of formal positive charge on the metal center. The other bands observed in the absorption spectra, near 295, 320, and 420 nm and in the range 490–540 nm, must be LMCT in origin, since their intensity is too high for ligand field transitions of high-spin Fe(III) complexes.[20] The visible band and that near 320 nm have been assigned to charge-transfer transitions from phenolate to iron(III);[6] the other bands remain to be assigned.

The visible band of the present iron(III) complexes shifts to higher energy on addition of ligand molecules to their solutions, while the rest of the spectrum seems less affected, at least when further absorptions by the added ligands are negligible. Some significant data obtained in methanol solutions are collected in Table II. Spectrophotometric titrations with imidazole as the added ligand show that two base molecules bind to Fe(sal-L-val)Cl, but only one binds to Fe(sal-L-his)Cl. In general, adduct formation is accompanied by a modest change in the intensity of the visible band, but for some ligands (e.g. benzoate, phenolate, and catecholate) a marked hyperchromic effect can also be observed. This is particularly evident for complexes of types **1** and **3**, while for **2** adduct formation may be incomplete. Binding of catecholate ligands to iron(III) produces additional charge-transfer bands in the visible region. This is shown in Figures 1 and 2 for representative complexes.

Table III. ESR Spectral Data for the Iron(III) Complexes

compound	CH_3CN/298 K		CH_3OH/123 K	
	g	ΔH_{pp}, G	*g*	ΔH_{pp}, G
Fe(sal-L-ala)Cl	2.015	52	4.15	176
Fe(sal-L-val)Cl	2.014	58	4.21	152
Fe(sal-L-phe)Cl	2.015	54	4.16	178
Fe(sal-L-his)Cl	2.014	50	4.18	196
Fe(sal-him)Cl_2	2.014	59	4.22	100

The visible CD spectra of complexes of type **1** exhibit a marked increase of CD activity on adduct formation. Two positive CD bands near 450 and 530 nm develop in all cases, but unlike the optical spectra these bands are little sensitive to the nature of the added ligand. For **2** the visible CD spectrum is much less affected by the addition of other ligand molecules; however, with salicylate and also thiosalicylate as the anions an inversion of the CD bands at 450 nm is observed. The lower energy portion of the CD spectra of Fe(sal-L-aa)Cl complexes also displays some changes upon binding of other ligands; the most notable general effect is an increase of negative CD activity for the shoulder at 420 nm, but changes occur also in the 300-nm region. Finally, it is worth noting that in no case did we observe racemization of the complexes in the presence of excess of an added base; in particular the imine CD band near 350 nm tended to increase, rather than decrease, its optical activity.

ESR Spectra. Powder samples of the Fe(sal-L-aa)Cl complexes exhibit broad (500–1500 G) ESR signals near $g = 4.3$ and $g = 2.0$ at room temperature. The relative intensity of these two signals varies from complex to complex, but it was actually found to vary to some extent also for different preparations of the complexes. While fluid methanol solutions of the complexes are ESR silent, those in acetonitrile exhibit a symmetrical and relatively sharp ESR signal near $g = 2.0$ (Table III). The intensity of this signal shows a reversible temperature effect: it decreases on lowering the temperature and almost completely disappears at the freezing point of the solutions ($\sim$225 K), but the signal appears again as the temperature is raised above the freezing point. Interestingly, this $g \sim 2.0$ signal disappears when a donor base like pyridine, imidazole, of α,α'-bipyridyl is added to the acetonitrile solutions of the complexes.

Frozen solutions of the iron(III) complexes exhibit the characteristic ESR signal near $g = 4.3$ predicted for a transition between the middle Kramers doublet of rhombically distorted, high-spin Fe(III) complexes[22] (Table III). An additional weak

(20) Lever, A. B. P. *Inorganic Electronic Spectroscopy* 2nd ed.; Elsevier: Amsterdam, 1984; p 452.
(21) For the adducts of Fe(sal-L-phe)Cl with nitrogen bases the positive CD activity develops only in times on the order of a few hours in dilute solution.
(22) (a) Oosterhuis, W. T. *Struct. Bonding (Berlin)* **1974**, *20*, 59–99. (b) Scullane, M. I.; White, L. K.; Chasteen, N. O. *J. Magn. Reson.* **1982**, *47*, 383–397. (c) Aasa, R. *J. Chem. Phys.* **1970**, *52*, 3919–3930. (d) Lang, G.; Aasa, R.; Garbett, K.; Williams, R. J. P. *Ibid.* **1971**, *55*, 4539–4548.

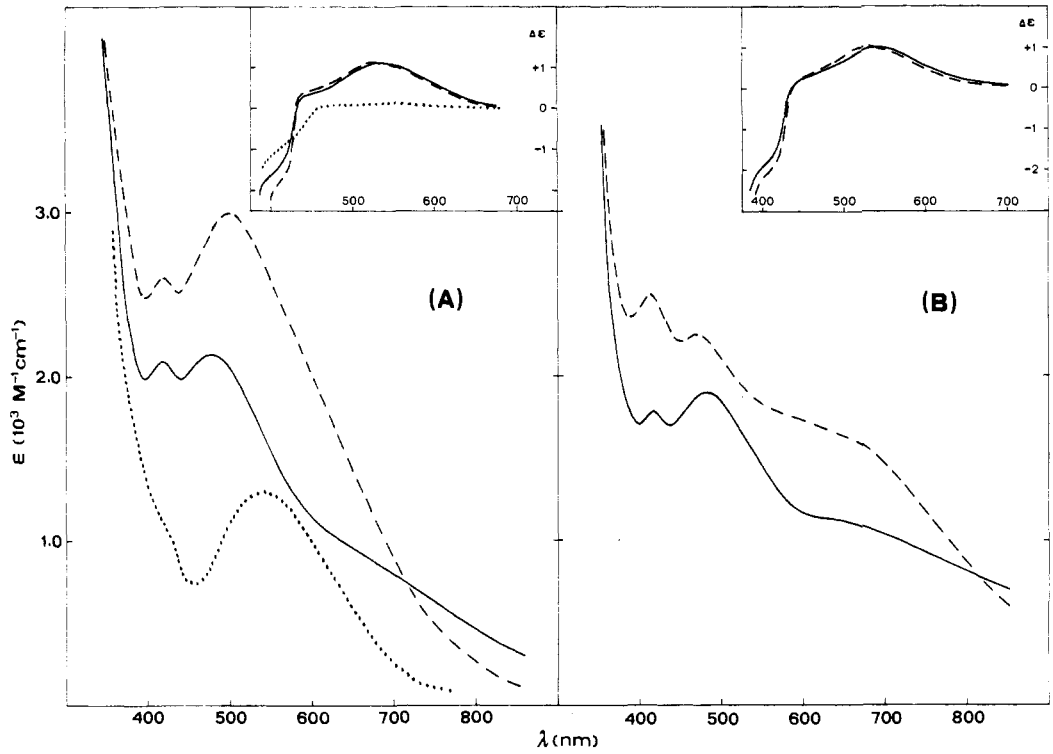

Figure 1. Optical spectra in dry methanol: (A) [Fe(sal-L-phe)(catH)] (solid line), generated anaerobically from Fe(sal-L-phe)Cl with 1 equiv of catechol and potassium *tert*-butoxide, and K[Fe(sal-L-phe)(cat)] (dashed line), generated anaerobically from Fe(sal-L-phe)Cl with 1 equiv of catechol and 2 equiv of potassium *tert*-butoxide; (B) [Fe(sal-L-phe)(dbcatH)] (solid line), generated anaerobically from Fe(sal-L-phe)Cl with 1 equiv of 3,5-di-*tert*-butylcatechol and potassium *tert*-butoxide, and K[Fe(sal-L-phe)(dbcat)] (dashed line), generated anaerobically from Fe(sal-L-phe)Cl with 1 equiv of 3,5-di-*tert*-butylcatechol and 2 equiv of potassium *tert*-butoxide. The spectrum of Fe(sal-L-phe)Cl (dotted line) is reported for appropriate comparison. The inserts show the visible CD spectra corresponding to the various complexes.

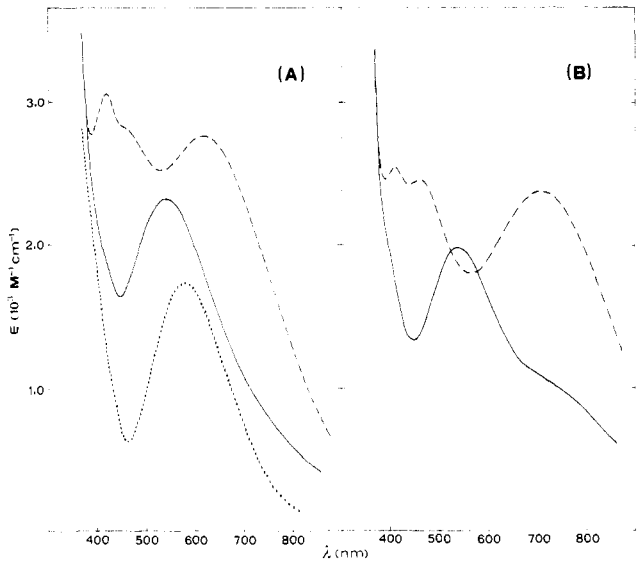

Figure 2. Optical spectra in dry methanol: (A) [Fe(sal-him)(catH)]Cl (solid line), generated anaerobically from Fe(sal-him)Cl_2 with 1 equiv of catechol and potassium *tert*-butoxide, and [Fe(sal-him)(cat)] (dashed line), generated anaerobically from Fe(sal-him)Cl_2 with 1 equiv of catechol and 2 equiv of potassium *tert*-butoxide; (B) [Fe(sal-him)(dbcatH)]Cl (solid line), generated anaerobically from Fe(sal-him)Cl_2 with 1 equiv of 3,5-di-*tert*-butylcatechol and potassium *tert*-butoxide, and [Fe(sal-him)(dbcat)] (dashed line), generated anaerobically from Fe(sal-him)Cl_2 with 1 equiv of 3,5-di-*tert*-butylcatechol and 2 equiv of potassium *tert*-butoxide. The spectrum of Fe(sal-him)Cl_2 (dotted line) is reported for appropriate comparison.

signal to low field of the main ESR signal is often observed; this may originate from a transition between another Kramers doublet.[22c] The line width of the $g \sim 4.3$ signal varies appreciably among the complexes and shows some solvent dependence. Adduct formation with various ligand molecules also affects this ESR signal; for instance, the line width decreases for complexes of type **1** and **2** in the presence of a donor base, but it tends to increase for **3**. Though, the signal is often asymmetric and also its intensity appears affected in the spectra of the various adducts.

NMR Spectra. The proton NMR spectra of the iron(III) complexes of type **1** recorded in various solvents show two sets of signals that can be attributed to two species in equilibrium in solution. The relative intensity of the signals corresponding to the two species depends markedly on the solvent and, to some extent, also on the concentration of the complex, while temperature effects are only marginal in the range 300–330 K. For one set of signals the magnitude of the NMR shifts and the pattern of the resonances resemble those observed for the phenyl protons of salicylaldimine residues of high-spin Fe(salen)X complexes.[8be,23,24] For instance, the most upfield shifted resonance is severalfold broader than the other signals, and it is therefore straightforward to assign it to the proton ortho to the phenolate oxygen atom. Occasionally we observed additional broad signals considerably downfield of the other signals that may be due to the azomethine and/or α-CH protons.[23] The second species exhibits signals with NMR shifts smaller by 15–30 ppm, but the magnitude of the shifts is still much higher than for low-spin complexes.[23] We tentatively assign also these signals to salicylaldimine protons, assuming the same alternating shift pattern as for Fe(salen)X complexes, since this pattern has been proven to be valid even for low-spin complexes of the same type.[23] Note that the 3-H signal of the species with smaller NMR shifts apparently overlaps with the 5-H signal of the species with larger NMR shifts. The line widths of the signals are generally much larger than those of Fe(salen)X complexes; this is probably the result of exchange contributions, because otherwise the magnetic coupling would lead to a sharpening of the NMR signals.[25] In

(23) La Mar, G. N.; Eaton, G. R.; Holm, R. H.; Walker, F. A. *J. Am. Chem. Soc.* **1973**, *95*, 63–75.
(24) Fanning, J. C.; Resce, J. L.; Lickfield, G. C.; Kotun, M. E. *Inorg. Chem.* **1985**, *24*, 2884–2889.

Table IV. Proton NMR Data for the Iron(III) Complexes[a]

system	solvent	species[b]	chem shifts, δ				
			ring protons				
			3-H	4-H	5-H	6-H	others
Fe(sal-L-ala)Cl	CD_3OD	M[c]	−95	80	−77	48	200[d]
		m		65	−52	25	
Fe(sal-L-val)Cl	CD_3OD	M	−90[d]	81	−77	52	250[d]
		m		67	−53	37	
	CD_3CN	M	−67	71	−52	43	
		m		78		52	
Fe(sal-L-phe)Cl	CD_3OD	M	−90[d]	82	−77	48	
		m		66	−53	32	
	CD_3CN	M	−76	72	−55	32	
		m		83		43	
Fe(sal-L-his)Cl	CD_3OD		−74	64	−48	35	−42
				81		45	
Fe(sal-him)Cl_2[e]	CD_3OD		−108	93	−94	60	73
+im	CD_3OD		−80[d]	81	−62	54	73, 46, 32, −38
+py	CD_3OD		−93	82	−63	57	72, −41
+bpy	CD_3OD		−92	84	−64	55	109, 98, 72, 43, 25
+dbcatH^-[f]	CD_3OD		−80[d]	80	−65	57	73, 44, 25,[d] −12, −38[d]
+dbcat^{2-}[f]	CD_3OD		−50[d]	54	−33	36	48, 29, −25

[a] All shifts are relative to Me_4Si with downfield shifts taken as positive. [b] M = major species; m = minor species. [c] Line width for the resonances (Hz): ~2000 (3-H); 500 (4-H); 900 (5-H); 600 (6-H). [d] Broad. [e] Line width for the resonances (Hz): ~1400 (3-H); 300 (4-H); 400 (5-H); 350 (6-H); 450 (δ 73 peak). [f] Recorded under nitrogen.

general, the species with larger NMR shifts is dominant in protic solvents (CD_3OD, D_2O) while that with smaller NMR shifts is dominant in nonprotic solvents (CD_3CN, $CDCl_3$, acetone-d_6). Some significant NMR data are collected in Table IV.

The NMR spectrum of Fe(sal-L-his)Cl in CD_3OD or D_2O is more difficult to interpret; the poor solubility of the complex prevented NMR investigation in less polar solvents. The spectrum may be interpreted as arising from two species (with larger and smaller NMR shifts) present in comparable amounts. However, an additional resonance at 42 ppm upfield, which is not observed in the spectra of the other complexes and overlaps considerably with one of the resonances, has no apparent counterpart if it is assigned to one of the two species. By contrast, the NMR spectrum of Fe(sal-him)Cl_2 in CD_3OD clearly shows a single species with resonances markedly sharper than those of the other complexes. The NMR shifts are 10–20 ppm larger than those of the Fe(sal-L-aa)Cl complexes, and an additional signal at 73 ppm downfield may possibly be assigned to the imidazole 5-H proton of the histamine residue.[5c]

The addition of donor ligands to solutions of the Fe(sal-L-aa)Cl complexes produces changes in the NMR spectra, often with the appearance of new signals that may be due to the coordinating ligands. In general, a marked reduction in the magnitude of the NMR shifts of the salicylaldimine protons is observed. However, the resulting signals have paramagnetic shifts comparable with those of the species with reduced NMR shifts of the original complexes, thus complicating accurate analysis of the spectra at this stage, since possible contributions from equilibria between, e.g., monomeric and dimeric species cannot be excluded, particularly for the adducts with monodentate ligands. This problem is more serious here than, for instance, in the analysis of the electronic spectra, where it is possible to operate in much more dilute solutions. The best systems for investigating the effect on the NMR spectra of binding of ligands to Fe(III) are those derived from Fe(sal-him)Cl_2, which give relatively sharp and often multiple resonances for the coordinated ligands (Table IV). The salicylaldimine protons undergo reduction in their NMR shifts in all cases, but the assignments given in Table IV are only tentative and need to be confirmed by more thorough analysis; representative spectra for the 3,5-di-*tert*-butylcatecholate adducts of Fe(sal-him)$^{2+}$ are shown in Figure 3.

MO Calculations. A discussion of the optical spectra of the iron(III) complexes in terms of phenolate–Fe(III) LMCT nec-

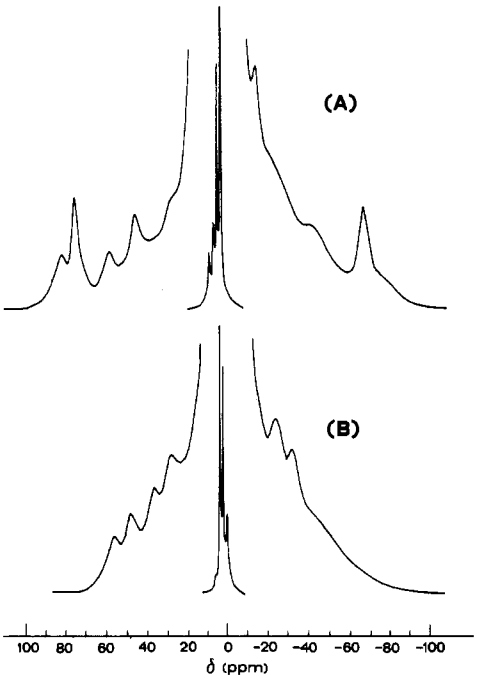

Figure 3. 80-MHz ^1H NMR spectra in dry CD_3OD: (A) [Fe(sal-him)(dbcatH)]Cl, generated anaerobically from Fe(sal-him)Cl_2 with 1 equiv of 3,5-di-*tert*-butylcatechol and potassium *tert*-butoxide; (B) [Fe(sal-him)(dbcat)], generated anaerobically from Fe(sal-him)Cl_2 with 1 equiv of 3,5-di-*tert*-butylcatechol and 2 equiv of potassium *tert*-butoxide. The concentration of the iron complex is about 10^{-2} M in both cases.

essarily must consider minimally the electronic structure of the free ligands and the possible interactions between ligand and metal orbitals. In order to gain an appreciation of the relation between the salicylaldimine chromophore and a nonconjugate phenolate chromophore such as that of the tyrosine residue present in the proteins, we performed MO calculations on the *N*-methylsalicylaldiminate (salme$^-$, **4**) and *p*-methylphenolate (cres$^-$, **5**)

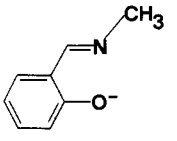

4

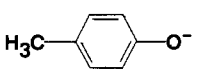

5

(25) Bertini, I.; Luchinat, C. *NMR of Paramagnetic Molecules in Biological Systems*; Benjamin Cummings: Boston, 1986.

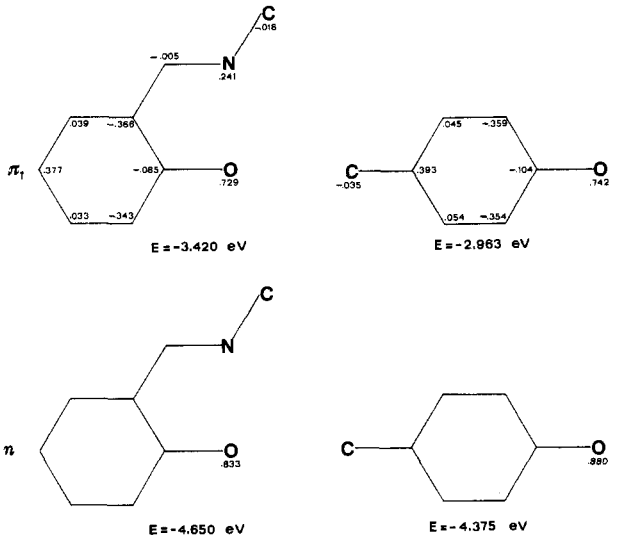

Figure 4. MO coefficients and energies of the two highest occupied molecular orbitals for the *N*-methylsalicylaldiminate and *p*-methylphenolate anions.

anions. The calculations were carried out according to the CNDO/2 scheme;[26] standard bond lengths and valence angles were derived from experimental data for similar molecules.[27] Diagrams reporting the relevant MO coefficients and energies are shown in Figure 4. Two orbitals are most important for the qualitative discussion of the optical spectra of iron phenolate complexes: the HOMO of π symmetry (π_1) and the occupied MO immediately below the HOMO. The MO coefficients reported in Figure 4 show that for both the salme$^-$ and the cres$^-$ anions the two orbitals considered have the largest amplitude around the oxygen atom. The second orbital, in particular, can be classified as a nonbonding orbital (n), since it is mainly composed of a linear combination of oxygen p orbitals leading to a σ orbital nearly orthogonal to the σ component of the C–O bond. The other occupied MOs are far removed in energy from π_1 and n: for salme$^-$, a σ-type orbital at −7.148 eV and a π orbital (π_2) at −7.382 eV; for cres$^-$, a σ-type orbital at −6.778 eV and π_2 at −8.432 eV. These orbitals can be neglected in the discussion of the low-energy phenolate–iron(III) LMCTs.

Discussion

Characterization and Spectral Assignments. In the iron(III) chelates of types **1** and **3**, the ligands provide three equatorial donor atoms, while in the histidine complex **2**, an additional donor group can bind to the iron(III) center in an axial position. As for the corresponding complexes with divalent metal ions[16-18] and other iron(III) chelates with tridentate salicylaldimine ligands,[28] it is expected that the molecular formulation of the present complexes involves at least dinuclear species. Assuming that the chloride ions are coordinated in the solid state, the iron(III) centers can achieve five- or six-coordinate structures by binding to polar groups of neighboring molecules. Except for Fe(sal-him)Cl_2, some degree of association is maintained in solution, and although we have no direct indication of the degree of association of the complexes, it seems reasonable to assume that we are dealing with equilibria between two species; these will be referred to as the monomer and the dimer. The amount of each species at equilibrium differs for the various complexes and depends markedly on the solvent (protic solvents favoring the cleavage of the clusters) and the presence of externally added ligands (that also favor the monomeric species). The chloride ions are quite certainly not coordinated in polar solvents, at least for the monomeric species.

An indication on the nature of the two species in solution is obtained from the ESR and NMR spectra of the complexes. While the ESR signals at $g \sim 4.2$ observed in frozen solutions are quite certainly associated with the monomeric species, those found near $g = 2.0$ in fluid solutions can be interpreted as arising from spin–spin-coupled, dinuclear iron species ($S_1 = S_2 = {}^5/_2$).[29] The ground state of the dimer is diamagnetic ($S' = 0$) and it is the only one populated at low temperature, but transitions in the dimer excited states ($S' = 1, 2, 3, 4, 5$), giving rise to ESR signals with $g = 2.0$, can occur as the temperature is raised. In this model the population increase of dimer excited states should be larger than the decrease of dimer concentration due to dissociation at the higher temperatures.[30] The existence of monomer–dimer equilibria for the Fe(sal-L-aa)Cl complexes is also evidenced by their NMR spectra, where signals belonging to the two species can be observed. Since spin–spin coupling in the dimer reduces the overall paramagnetism of the complexes, we can assign the set of NMR signals with smaller NMR shifts to the dimeric species and that with larger NMR shifts to the monomeric species.

The CD spectra provide information on the stereochemical features of the complexes. As we have discussed in detail elsewhere,[16-18] the metal center of *N*-salicylidene-L-amino acidato complexes generally have five- or six-coordinate structures, and it is likely that such structures are maintained in the present iron(III) complexes. The experiments carried out in the presence of added bases show that for systems of type **1** only two coordination positions (one axial and one equatorial) are available to the added base. Coordination of an additional molecule of base in the second axial position can be excluded because it may occur only with concomitant inversion of the amino acid chelate ring to the unfavorable conformation carrying a pseudoequatorial side chain.[16-18] This arrangement would be revealed by an inversion of sign of the imine CD band since this is sensitive to the conformation of the chelate ring.[17b] For the parent, optically silent zinc(II) complexes, we recently concluded that the relationship between sign of the imine CD band and ring conformation arises because the mechanism leading to the optical activity within this band is electric dipole–dipole coupling between the transition moments of the imine and one of the $\pi \rightarrow \pi^*$ transitions of the carboxylate group.[31] The spatial arrangement of these transition moment vectors leads to opposite chirality for the two conformations of the amino acid chelate ring. Although the presence of the iron(III) chromophore can in principle provide additional mechanisms for generation of optical activity within the imine band, it is likely that the above interaction remains dominant, since the CD intensity of the band is comparable for the iron(III) and zinc(II)[16] complexes.

In the case of the histidine complex **2**, a single donor molecule can bind to iron(III) in an equatorial position. Indeed, the absorption and CD spectra of, e.g., Fe(sal-L-val)Cl and Fe(sal-L-his)Cl in the presence of excess imidazole are remarkably similar throughout the spectral range. The differences in the intensities

(26) Klopman, G.; Evans, R. C. In *Semiempirical Methods of Electronic Structure Calculations*; Segal, G. A., Ed.; Plenum: New York, 1977; pp 29–67.

(27) Sutton, L. E., Phil, M. A. D., Eds. *Tables of Interatomic Distances and Configuration in Molecules and Ions*; The Chemical Society: London, 1958.

(28) (a) Van den Bergen, A.; Murray, K. S.; West, B. O.; Buckley, A. N. *J. Chem. Soc. A* **1969**, 2051–2060. (b) Bertrand, J. A.; Eller, P. G. *Inorg. Chem.* **1974**, *13*, 927–934. (c) Syamal, A.; Kale, K. S. *Indian J. Chem., Sect. A* **1980**, *19A*, 488–491.

(29) (a) Borer, L.; Thalken, L.; Ceccarelli, C.; Glick, M.; Zhang, J. H.; Reiff, W. M. *Inorg. Chem.* **1983**, *22*, 1719–1724. (b) Borer, L.; Thalken, L.; Zhang, J. H.; Reiff, W. M. *Ibid.* **1983**, *22*, 3174–3176. (c) Reid, A. F.; Perkins, H. K.; Sienko, M. J. *Ibid.* **1968**, *7*, 119–126. (d) Murray, K. S. *Coord. Chem. Rev.* **1974**, *12*, 1–35.

(30) An alternative interpretation of the $g \sim 2.0$ ESR signals involves the existence of low-spin species ($S_1 = S_2 = {}^1/_2$) in a monomer–dimer equilibrium. In this case the linear increase of signal intensity observed with temperature can be explained by enhanced dissociation of the dimer. However, this model does not explain the immediate and complete disappearance of the ESR signals for the low-spin monomeric species occurring on freezing or adding a donor base to the solutions, since the adducts with bases of low-spin complexes are also expected to be low spin. Moreover, the existence of low-spin species in solution seems excluded by the NMR spectra, where the various proton signals display paramagnetic shifts by far larger than expected for low-spin complexes.[23]

(31) Casella, L.; Gullotti, M. *J. Am. Chem. Soc.* **1983**, *105*, 803–809.

of the various bands observed in these spectra are due only to imidazole chelation in the histidine complex. Even with potentially chelating bases like α,α'-bipyridyl or *o*-phenylenediamine the spectral evidence is in favor of monodentate binding to the Fe(sal-L-his)$^+$ residue (Table I). It is possible that a significant displacement of iron(III) from the equatorial plane toward the imidazole group in **2** does not allow more than weak binding of the chelating base in the axial position trans to the imidazole group. A comparison of the CD spectra of complexes of type **1** with that of **2** or those of **1** + base also shows clearly that the appearance of optical activity in the visible region is associated with coordination of a donor molecule in the axial position. The behavior of the histamine complex **3** parallels that of the amino acid complexes of type **1**; the flexibility of the six-membered histamine ring is expected to facilitate binding of additional donor ligands.

The optical spectra of the complexes are largely determined by electronic transitions originating within the iron salicylaldiminate chromophore. The MO calculations performed on the anions **4** and **5** show that the phenolate orbitals that can be involved in low-energy LMCT transitions have similar symmetry and energy. This result warrants that the information obtained on the iron salicylaldiminate chromophore can be transferred to the parent iron tyrosinate chromophore. The low-energy LMCT transitions observed in the spectra of the present iron(III) complexes can thus be discussed in terms of the ligand π_1 and n orbitals (Figure 4). As proposed by others,[6] the visible band in the 500-nm region can be assigned to a transition from π_1 to an iron d_π orbital of proper symmetry (e.g. d_{xz}). This transition should be red shifted in the corresponding iron phenolate chromophore in view of the higher stability of the ligand π_1 orbital in **4** compared to **5**, but of course the position of this band in the two iron systems depends upon the relative magnitude of the π_1–d_π bonding interactions, which are difficult to assess. The next band in order of increasing energy occurs near 420 nm. This probably corresponds to electron excitation from π_1 to a higher energy orbital of the split t_{2g} set, since its energy separation from the 500-nm band seems too small (3000–4000 cm^{-1}) to assign it to LMCT from π_1 to an orbital of the e_g set. At still higher energy there are two other LMCT bands near 295 and 320 nm. Previously, for an octahedral iron–salicylaldimine complex, a band at 315 nm has been assigned to $\pi_1 \rightarrow d_\sigma$ LMCT transition.[6] The two absorptions near 300 nm of the present complexes can thus be attributed to LMCT from π_1 to the split e_g orbitals. However, an alternative assignment involving the phenolate n orbitals, hence n $\rightarrow d_\pi$ LMCT, cannot be discarded on energy grounds, since the energy separation between the bands near 300 and 500 nm is of the same order of magnitude as the energy difference between the ligand π_1 and n orbitals.[32]

Further evidence for the assignments of the LMCT transitions is obtained by considering the CD spectra of the complexes and the effect of binding additional donor molecules to iron(III). In general, while more or less pronounced optical activity is associated with the absorptions near 420 nm and in the 300-nm region, the band near 500 nm is apparently not dichroic. This provides support for the $\pi_1 \rightarrow d_\pi$ assignment, since such excitation does not involve rotation of charge. All the CD activity developed above ~450 nm is probably associated with d–d transitions; it may be enhanced on binding an axial ligand to iron(III) by the lowering of symmetry of the complex that results from displacement of the metal from the coordination plane. Octahedral iron(III)–amino acid complexes, in fact, display extremely weak optical activity in the visible region.[33] The band near 420 nm is weaker than that near 500 nm, but its intensity and optical activity are larger for **2** than for complexes of type **1** and increase systematically in the latter systems on binding an axial ligand. By contrast, the position of this band is little affected by the axial ligand; thus, if it is $\pi_1 \rightarrow d_\pi$ LMCT in origin, the d orbital involved is probably d_{xy}. Arguments based on orbital overlap seem consistent with this interpretation: d_{xy} and π_1 are orthogonal when the metal lies in the equatorial coordination plane; for this arrangement we thus expect low intensity and optical activity for the $\pi_1 \rightarrow d_{xy}$ transition. The CD activity in the 300-nm region is more variable and may be partly canceled by the more intense adjacent imine and aromatic CD bands. However, the intensity of the absorption bands near 295 and 320 nm is higher than that corresponding to the $\pi_1 \rightarrow d_\pi$ transitions, so we should expect a more efficient overlap between the orbitals involved. Assignments like n $\rightarrow d_\sigma$ LMCT would thus be preferable for these bands than either $\pi_1 \rightarrow d_\sigma$ or n $\rightarrow d_\pi$, but this seems precluded on energy grounds.

Of the donor groups other than phenolate that are present in **1–3**, only the imidazole group of **2** and **3** needs to be taken into account for low-energy LMCT transitions, since LMCT transitions originating from the carboxylate group are expected to give minor contributions to the near-UV spectrum.[34] Detailed studies on imidazole to iron(III) LMCT transitions are currently limited to low-spin complexes.[35] The lowest energy LMCT band for [Fe(CN)$_5$im]$^{2-}$, π_1(im) $\rightarrow d_\pi$, occurs near 475 nm ($\epsilon < 500$ M^{-1} cm^{-1}) and is followed by a more intense LMCT band, π_2, n(im) $\rightarrow d_\pi$, near 400 nm ($\epsilon > 1000$ M^{-1} cm^{-1}).[35] For the present high-spin complexes these LMCT bands should be found at higher energy and are probably buried under more intense absorptions.

Relevance to Iron Tyrosinate Proteins. An important feature of model studies of these and other iron(III) salicylaldiminate complexes is the sensitivity of the phenolate to iron(III) charge-transfer band to the ligand environment of the metal center. Even though the numerical data reported in Table II should be taken only as indicative, for the possible complications arising from incomplete adduct formation and monomer–dimer equilibria, some trends are apparent. Addition of any donor molecule shifts the visible LMCT band to higher energy; this effect is to be ascribed to the raise in energy of the metal orbitals resulting from the increased electron density at the metal center.[36] When the ligand is imidazole, we observe a relatively constant hypsochromic shift of 2000 cm^{-1} for binding of two donor molecules to either **1** or **3**. However, the effect of binding the first imidazole in an axial position (1200–1500-cm^{-1} shift) is larger than that of the second imidazole in an equatorial position (500–800-cm^{-1} shift), as is confirmed by the data obtained for **2**. With ligands containing phenolate groups the blue shift of the iron salicylaldiminate LMCT band is accompanied by an increase in absorptivity. This is due to the occurrence of additional LMCT transitions from the added ligand to iron(III) at similar energies. The effect is maximum for chelating ligands like salicylate and catecholate; for the anions of the catechol derivatives, in particular, the additional absorptions, due to catecholate to iron(III) LMCT transitions, often occur as separate bands (see also Figures 1 and 2).

The CD spectra of the complexes show that binding of an axial donor group to iron(III) results in an increase of CD activity in the visible region, but there is no indication that such optical activity is associated to a noticeable extent with the phenolate to iron(III) LMCT transition. The situation in the proteins is more involved since in some cases the visible CD extremum is close to the absorption maximum,[37] while in other cases there is no apparent correspondence between the two spectra.[4a,38] In general,

(32) It is worth noting that although the present discussion of the phenolate to iron(III) LMCT transitions assumes the conventional energy ordering of the orbitals in which the filled ligand orbitals are more stable than the metal d orbitals, the actual energies of the highest occupied phenolate ligand orbitals may be comparable with that of the iron d orbitals. Under these conditions, a more advanced treatment, with inclusion of the d–d Coulomb interaction, would be required for a detailed discussion of the optical transitions.

(33) Puri, R. N.; Asplund, R. O.; Turker, W. F. *Inorg. Chim. Acta* **1982**, *66*, 7–11.

(34) (a) Schugar, H. J.; Rossman, G. R.; Barraclough, C. G.; Gray, H. B. *J. Am. Chem. Soc.* **1972**, *94*, 2683–2690. (b) Puri, R. N.; Asplund, R. O. *Inorg. Chim. Acta* **1982**, *66*, 49–56.

(35) Johnson, C. R.; Henderson, W. W.; Shepherd, R. E. *Inorg. Chem.* **1984**, *23*, 2754–2763.

(36) (a) Reference 20; pp 710–720. (b) Lever, A. B. P. *J. Chem. Educ.* **1974**, *51*, 612–616.

(37) (a) Nagy, B.; Lehrer, S. S. *Arch. Biochem. Biophys.* **1972**, *148*, 27–36. (b) Mazurier, J.; Aubert, J.-P.; Loucheux-Lefevre, M.-H.; Spik, G. *FEBS Lett.* **1976**, *66*, 238–242.

however, all these protein CD bands are broad and diffuse like those observed here for the iron complexes and their adducts. In addition, the protein CD spectra exhibit well-resolved bands in the 300–330-nm region that are also associated with the iron phenolate chromophores but are generally not apparent or resolved in the absorption spectra, where they are buried under the tail of much more intense protein absorptions. Perhaps we can note the absence of protein absorptions or CD features in the range 400–420 nm, where the present iron salicyladiminate complexes exhibit definite absorption and optical activity. These optical features may depend on the actual geometry of iron(III) and be displaced at different energy in the protein spectra; for instance, these spectra often show CD bands near 380 nm that may have a similar origin.[37,38]

The spectra of the catecholate adducts of the iron complexes deserve further comment in view of their possible relevance as mimics for the enzyme–substrate complexes of the catechol dioxygenases.[4] Indeed, several of the visible spectra of the adducts with catecholate anions, particularly those we formulate, e.g. as [Fe(sal-L-aa)(catH)], bear a striking similarity to the spectra of the enzyme complexes.[4] Even though this correspondence may be fortuitous, there are a few more general features of the spectra that are worth of note: (i) binding of catecholate anions to iron(III) results in increased absorptions both near 700 nm (the region of catecholate to iron(III) LMCT transitions[8a]) and between 400 and 500 nm (the region of phenolate to iron(III) LMCT transitions); (ii) like the phenolate to iron(III) LMCT, the catecholate to iron(III) LMCT transitions are also not dichroic; (iii) the spectra of the adducts with the catecholate monoanion ($catH^-$) differ from those of the adducts with the dianion (cat^{2-}), as is particularly evident for the adducts of the complex Fe(sal-him)Cl_2 (Figure 2).

The first observation implies a comment on the spectra of the enzyme–substrate complexes of the catechol dioxygenases in steady-state conditions, since these invariably show the appearance of distinctive absorptions near 700 nm but show a negligible increase, or even a slight decrease, of absorption in the region of the phenolate to iron(III) LMCT transitions.[4,39] It seems difficult to account for the optical spectra of these enzyme adducts without assuming that catechol binding occurs with concomitant displacement of one of the bound tyrosine residues. This conclusion is admittedly in conflict with resonance Raman studies carried out on the enzyme–substrate complexes[2] and may thus require further evidence from model studies, but indeed the increase of absorption between 400 and 500 nm observed here on catechol binding is remarkable. On the other hand, the lack of optical activity within the catecholate to iron(III) LMCT transitions suggests that the changes occurring in the CD spectra of the enzymes on substrate binding[4a,37] must be attributed to some structural changes occurring at the iron sites.

The third point raises the question of the mode of binding of the catecholate anions to the complexes. These anions are good chelating ligands for iron(III),[40] and from molecular models it is apparent that there is no particular hindrance to bidentate binding to systems of types **1–3** even for the sterically encumbering 3,5-di-*tert*-butylcatecholate anions. We thus are able to exclude monodentate binding of catecholate anions, such as that found for the adduct of the iron(III) complex of *o*-phenylenebis(salicylideneaminate),[9a] occurring in the present complexes. A more serious problem can be the distinction of the protonated species, e.g. [Fe(sal-L-aa)(catH)], from those nonprotonated, e.g. [Fe(sal-L-aa)(cat)]$^-$, since their separate existence in solution may not be evident.[40b] Except for Fe(sal-L-his)Cl, the optical spectra that we associate with the two species seem sufficiently different from each other to enable the current assignment, but it is also true that such differences become less evident for the adducts of complexes of type **1** with the 3,5-di-*tert*-butylcatecholate anions. Further investigation by NMR spectroscopy should provide additional evidence on the nature of these adducts, as has been shown for those of Fe(salen)X complexes[8b] and seems confirmed here by the spectra of [Fe(sal-him)(dbcatH)]$^+$ and [Fe(sal-him)(dbcat)] reported in Figure 3. The mode of binding of catechol anions to iron(III) is important in relation to the mechanism of oxidative cleavage of catechols by non-heme iron dioxygenases.[8c] Preliminary experiments carried out with Fe(sal-him)Cl_2 show that the complex is catalytically active in the oxidation of di-*tert*-butylcatechol by dioxygen at a very low Fe/catechol molar ratio (2/100) and under mild conditions (acetonitrile solution, room temperature, reaction times on the order of a few hours). Among the reaction products, which include 3,5-di-*tert*-butyl-1,2-benzoquinone and the oxygenation product 3,5-di-*tert*-butyl-2-hydroxy-1,4-benzoquinone, we have identified the oxidative-cleavage product 3,5-di-*tert*-butyl-1-oxacyclohepta-3,5-diene-2,7-dione. These results encourage further investigation of the present iron complexes as models for the reactivity of the catechol dioxygenases.

Acknowledgment. This work was supported by the Italian CNR. We are indebted to Professor P. Fantucci for the MO calculations and Professors I. Bertini and C. Luchinat for a helpful discussion of the NMR data. We thank one of the reviewers for drawing our attention to the signs of the MOs. The magnetic susceptibilities were measured by M. S. Franzoni, and the NMR spectra obtained in Milano were recorded by M. Bonfà.

Registry No. **4**, 57514-65-5; **5**, 22113-51-5; Fe(sal-L-ala)Cl, 106799-66-0; Fe(sal-L-val)Cl, 106799-67-1; Fe(sal-L-phe)Cl, 106799-68-2; Fe(sal-L-his)Cl, 106799-69-3; Fe(sal-him)Cl_2, 106799-70-6; Fe(sal-L-val)(bpy)Cl, 106799-71-7; Fe(sal-L-his)(bpy)Cl, 106799-72-8; Fe(sal-L-val)$(im)_2$Cl, 106799-73-9; Fe(sal-L-his)(im)Cl, 106799-74-0; [Fe(sal-L-phe)(catH)], 106799-75-1; K[Fe(sal-L-phe)(cat)], 106862-46-8; [Fe(sal-L-phe)(dcatH)], 106799-76-2; K[Fe(sal-L-phe)(dbcat)], 106862-47-9; [Fe(sal-him)(catH)]Cl, 106799-77-3; [Fe(sal-him)(dbcatH)]Cl, 106799-78-4; [Fe(sal-him)(cat)], 106820-76-2; [Fe(sal-him)(dbcat)], 106799-79-5; salicylaldehyde, 90-02-8; alanine, 56-41-7; valine, 72-18-4; phenylalanine, 63-91-2; histidine, 71-00-1; histamine, 51-45-6; catechol dioxygenase, 9027-16-1.

Supplementary Material Available: Listings of magnetic moments and complete IR data (Table IS) and electronic and CD spectral data in methanol of the iron complexes (Table IIS) (2 pages). Ordering information is given on any current masthead page.

(38) (a) Nakazawa, A.; Nakazawa, T.; Kotani, S.; Nozaki, M.; Hayashi, O. *J. Biol. Chem.* **1969**, *244*, 1527–1532. (b) Zaborsky, O. R.; Hou, C. T.; Ogletree, J. *Biochim. Biophys. Acta* **1975**, *386*, 18–25. (c) Antanaitis, B. C.; Strekas, T.; Aisen, P. *J. Biol. Chem.* **1982**, *257*, 3766–3770.

(39) (a) Bull, C.; Ballou, D. P.; Otsuka, S. *J. Biol. Chem.* **1981**, *256*, 12681–12686. (b) Bull, C.; Ballou, D. P. *Ibid.* **1981**, *256*, 12673–12680. (c) Whittaker, J. W.; Lipscomb, J. D.; Kent, T. A.; Münck, E. *Ibid.* **1984**, *259*, 4466–4475.

(40) (a) Pierpont, C. G.; Buchanan, R. M. *Coord. Chem. Rev.* **1981**, *38*, 45–87. (b) Lloret, F.; Moratal, J.; Faus, J. *J. Chem. Soc., Dalton Trans.* **1983**, 1749–1753.